The Journal of Neuroscience, June 15, 2001, *21*(12):4249–4258

BDNF Enhances Quantal Neurotransmitter Release and Increases the Number of Docked Vesicles at the Active Zones of Hippocampal Excitatory Synapses

William J. Tyler and Lucas D. Pozzo-Miller

Department of Neurobiology, University of Alabama at Birmingham, Birmingham, Alabama 35294-0021

Brain-derived neurotrophic factor (BDNF) is emerging as a key mediator of activity-dependent modifications of synaptic strength in the CNS. We investigated the hypothesis that BDNF enhances quantal neurotransmitter release by modulating the distribution of synaptic vesicles within presynaptic terminals using organotypic slice cultures of postnatal rat hippocampus. BDNF specifically increased the number of docked vesicles at the active zone of excitatory synapses on CA1 dendritic spines, with only a small increase in active zone size. In agreement with the hypothesis that an increased docked vesicle density enhances quantal neurotransmitter release, BDNF increased the frequency, but not the amplitude, of AMPA receptor-mediated miniature EPSCs (mEPSCs) recorded from CA1 pyramidal neurons in hippocampal slices. Synapse number, independently estimated from dendritic spine density and electron microscopy measurements, was also increased after BDNF treatment, indicating that the actions of BNDF on mEPSC frequency can be partially attributed to an increased synaptic density. Our results further suggest that all these actions were mediated via tyrosine kinase B (TrkB) receptor activation, established by inhibition of plasma membrane tyrosine kinases with K-252a. These results provide additional evidence of a fundamental role of the BDNF–TrkB signaling cascade in synaptic transmission, as well as in cellular models of hippocampus-dependent learning and memory.

Key words: active zones; CA1; dendritic spines; docked vesicles; hippocampus; mEPSCs; neurotrophins; synapses; TrkB receptors

Neurotrophins have been classically implicated in the survival and differentiation of specific populations of neurons within the CNS (Lewin and Barde, 1996). Recent evidence indicates that they also play fundamental roles in synaptic plasticity within brain regions relevant to learning and memory (Thoenen, 1995; McAllister et al., 1999; Schinder and Poo, 2000). Specifically, brain-derived neurotrophic factor (BDNF) has been shown to enhance glutamatergic synaptic transmission (Lessman et al., 1994; Levine et al., 1995; Lessman and Heumann, 1998; Li et al., 1998a,b; Schinder et al., 2000) and to modulate synaptic scaling of excitatory inputs (Rutherford et al., 1998) in primary cultures of embryonic hippocampal neurons. Knock-out mice lacking the *bdnf* gene exhibit deficits in long-term potentiation (LTP) (Korte et al., 1995; Patterson et al., 1996; Pozzo-Miller et al., 1999b), the most studied cellular model of associative learning (Bliss and Collingridge, 1993), whereas BDNF promotes LTP induction in hippocampal slices from developing rats (Figurov et al., 1996). Furthermore, mice with a conditional gene knock-out of the tyrosine kinase B (TrkB) BDNF receptor in the CA1 region during the second postnatal week show impairments in LTP (Minichiello et al., 1999; Xu et al., 2000), as well as in various hippocampus-dependent learning paradigms (Minichiello et al., 1999).

The observation that BDNF prevents synaptic fatigue in developing hippocampal slices (Figurov et al., 1996; Gottschalk et al., 1998) and in *bdnf* knock-out mice (Pozzo-Miller et al., 1999b) led to the hypothesis that BDNF may promote LTP induction by preventing synaptic fatigue induced by high-frequency LTP-inducing stimuli. Because the synaptic vesicle has been historically accepted as corresponding to individual quantal events in the classical description of neurotransmitter release at the neuromuscular junction (Katz, 1969), synaptic fatigue during sustained high-frequency stimulation has been proposed to result from depletion of the readily releasable pool of synaptic vesicles (Model et al., 1975; Dickinson-Nelson and Reese, 1983; Zucker, 1989; Dobrunz and Stevens, 1997). Recent three-dimensional reconstructions of hippocampal synapses *in vivo* and *in vitro* provide evidence supporting this idea, further suggesting that release probability is proportional to the number of synaptic vesicles docked at the active zone (Harris and Sultan, 1995; Schikorski and Stevens, 1997). In this report we used a combination of quantitative electron microscopy, whole-cell patch-clamp recording, immunocytochemistry, and confocal microscopy to test the hypothesis that BDNF enhances quantal neurotransmitter release in organotypic slice cultures of rat hippocampus by modulating the distribution of synaptic vesicle pools within presynaptic terminals.

MATERIALS AND METHODS

Organotypic slice cultures and experimental treatments. Transverse hippocampal slices (~500 μm thick) from postnatal day 7 Sprague Dawley

Received Feb. 6, 2001; revised March 7, 2001; accepted March 20, 2001.

This work was supported by National Institutes of Health (NIH) Grants RO1-NS40593-01 and PO1-HD38760 (L.D.P.-M.). We thank Amgen for the generous supply of BDNF; Drs. R. Llinás (New York University), J. Hablitz [University of Alabama at Birmingham (UAB)], R. Lester (UAB), and B. Lu (NIH) for advice and critical reading of this manuscript; Dr. K. Harris (Harvard Medical School) for sharing the protocol for microwave-enhanced fixation; Dr. T. Inoue (Tokyo University) for data acquisition software; E. Philips (Neurobiology Imaging Core, UAB) for excellent EM support; S. Haymon and M. Fisher for preliminary EM and confocal data acquisition and analysis; and the High Resolution Imaging Facility (UAB) for the use of the confocal microscope.

Correspondence should be addressed to Dr. Lucas Pozzo-Miller, Department of Neurobiology, CIRC-429, University of Alabama at Birmingham, 1719 6th Avenue South, Birmingham, AL 35294-0021. E-mail: pozzomiller@nrc.uab.edu.

rats (Harlan Sprague Dawley, Indianapolis, IN) were prepared with a custom-designed wire slicer and maintained *in vitro* on Millicell-CM filter inserts (Millipore, Bedford, MA) in a 36°C, 5% CO_2, humidified (99%) incubator (Stoppini et al., 1991; Pozzo-Miller et al., 1993). The concentration of horse serum (Life Technologies, Gaithersburg, MD) in the culture medium was reduced from 20 to 10% at 6 d *in vitro* (div) and again reduced to 5% 24 hr later. After 24 hr in medium containing 5% horse serum, slices were placed in serum-free medium [Neurocellular II (Biofluids, Rockville, MD) plus B-27 supplement (Life Technologies)] for 24 hr. Slice cultures were then treated with either (1) serum-free medium, (2) BDNF (250 ng/ml; Amgen, Thousand Oaks, CA) in serum-free medium, (3) K-252a (200 nM; Calbiochem, La Jolla, CA) for 24 hr before adding BDNF in conjunction with K-252a in serum-free medium, or (4) K-252a (200 nM) alone in serum-free medium. The culture medium was completely exchanged every 3 d. Slices were used for physiological recordings between 12 and 14 div or fixed on day 14 *in vitro* for laser-scanning confocal microscopy, immunocytochemistry, or electron microscopy.

Immunocytochemistry and laser-scanning confocal microscopy. Fourteen div slice cultures were fixed overnight in 4% paraformaldehyde in PBS, rinsed in PBS, incubated in blocking and permeabilization buffer (10% horse serum, 2% bovine serum albumin, and 0.1% Triton X-100 in PBS), and then incubated overnight (4°C) in one of the following primary antibodies: anti-TrkB (polyclonal; 1:250; Promega, Madison, WI), anti-synaptobrevin (polyclonal; 1:250; Santa Cruz Biotechnology, Santa Cruz, CA), anti-synaptophysin (polyclonal; 1:250; Santa Cruz Biotechnology), or anti-Ca^{2+}/calmodulin-dependent protein kinase II (anti-CaMKII; monoclonal; 1:250; Boehringer Mannheim, Indianapolis, IN). After incubation with biotinylated secondary antibodies (1:250; Santa Cruz Biotechnology), slices were treated with avidin-conjugated fluorescein or Texas Red (10 μl/ml; Vector Laboratories, Burlingame, CA), mounted and sealed with Vectashield (Vector Laboratories), and imaged with a laser-scanning confocal microscope (LSCM; Olympus Fluoview, Mellville, NY). Confocal images were acquired from the CA1 region using a dry 20× [0.8 numerical aperture (NA)] or oil-immersion 60× (1.2 NA) or 100× (1.65 NA) objective lenses (Olympus Fluoview). Appropriate controls lacking primary antibodies were performed for each one of the antibodies. To perform double immunostaining of presynaptic and postsynaptic proteins, slices were completely processed through the first series of reactions, rinsed, and followed by the second series of immunoreactions.

Microwave-enhanced transmission electron microscopy. Slice cultures were processed for transmission electron microscopy (EM) using microwave-enhanced fixation (Jensen and Harris, 1989; Shepherd and Harris, 1998). Fourteen div slice cultures were immersed in 6% glutaraldehyde and 4% paraformaldehyde in 0.1 M cacodylate buffer and fixed under microwave irradiation at 37°C for 8 sec in a laboratory microwave (Pelco 3450 Laboratory Microwave Processor; Ted Pella, Redding, CA). Slices were then kept overnight at room temperature in the same fixative. Slices were then placed in a reduced osmium solution (K-ferrocyanide and 1% OsO_4 in 0.1 M cacodylate buffer), cooled on ice, and then microwaved for 2.5 min at 37°C. After rinsing, the slices were placed in another osmium solution (1% OsO_4 in 0.1 M cacodylate buffer), cooled on ice, and again microwaved for 2.5 min at 37°C. The slices were then immersed in ice-cold 1% aqueous uranyl acetate, followed by microwave irradiation at 37°C for 2.5 min. After rinsing, slices were dehydrated in a graded acetone series (50, 70, 90, and 100%; two times each) at 37°C for 40 sec in the microwave. Slices were then flat-embedded in Poly/Bed 812 (Electron Microscopy Sciences, Fort Washington, PA) between plastic coverslips (Thermanox; Nunc, Naperville, IL) for 24 hr at 60°C. Semithin sections (0.5 μm) were cut, stained with toluidine blue, and used to locate and trim the CA1 stratum radiatum region. Ultrathin sections from CA1 stratum radiatum stained with uranyl acetate and lead citrate were examined in a Jeol-100CX transmission electron microscope operated at 80 kV (Jeol, Peabody, MA). Asymmetric synapses on dendritic spines were identified by their prominent electron-dense postsynaptic density, whereas spines were recognized by their size and/or shape, the continuity with the dendritic shaft, or the lack of microtubules and mitochondria.

Quantitative analysis of synapses by EM. To estimate the number of reserve and docked synaptic vesicles, individual asymmetric spine synapses within CA1 stratum radiatum were photographed at 33,000×, whereas estimates of synapse density and active zone length were performed by sampling random fields within CA1 stratum radiatum at 16,000× (total sampling area = 680 μm^2). The negatives were scanned, digitally inverted, and analyzed using NIH Image, as described previously (Pozzo-Miller et al., 1999b). To avoid size biases in the quantitative analysis of the distribution of synaptic vesicles within presynaptic terminals, only synapses having approximately equal presynaptic terminal area and active zone length were selected for quantitative analysis (ranges of active zone length in controls, 0.11–0.48 μm; in BDNF, 0.09–0.63 μm; in K-252a + BDNF, 0.16–0.46 μm; and in K-252a, 0.19–050 μm; ranges of preterminal areas in controls, 0.10–0.77 μm^2; in BDNF, 0.08–0.77 μm^2; in K-252a + BDNF, 0.10–0.55 μm^2; and in K252a, 0.13–0.61 μm^2). Only small clear synaptic vesicles (~50 nm) were counted when at least one-half of the circumference of their total plasma membrane was clearly present (Heuser and Reese, 1973; Pozzo-Miller et al., 1999b). Docked vesicles were defined as those within one vesicle diameter (~50 nm) of the presynaptic active zone (Dickinson-Nelson and Reese, 1983; Pozzo-Miller et al., 1999b). By use of the number of docked vesicles and the active zone length from the two-dimensional sections, the total number of docked vesicles (TDV) per active zone was estimated on the basis of published assumptions (Pozzo-Miller et al., 1999b).

Spontaneous miniature EPSC recording. Slice cultures were transferred to an immersion-type chamber continuously perfused (1 ml/min) with artificial CSF (aCSF) containing (in mM): NaCl 124, KCl 2, KH_2PO_4 1.24, $MgSO_4$ 1.3, $NaHCO_3$ 17.6, $CaCl_2$ 2.5, and D-glucose 10; the osmolarity was adjusted to 310 mOsm with sucrose. The aCSF was continuously bubbled with 95% O_2/5% CO_2. Recordings were made at room temperature with pipettes filled with a solution containing (in mM): K^+-gluconate 120, KCl 17.5, NaCl 10, Na-HEPES 10, EGTA 0.2, Mg-ATP 2, Na-GTP 0.2, and QX-314 20, at 280–290 mOsm and pH 7.2. The final resistance of the unpolished patch electrodes filled with this intracellular solution was 8–10 MΩ. Whole-cell voltage-clamp recordings were made from visually identified CA1 pyramidal neurons using a 63× (0.9 NA) water-immersion objective (Achroplan; Zeiss, Thornwood, NY) on a fixed-stage upright microscope (Zeiss Axioskop FS) using differential interference contrast- and infrared-imaging techniques, as described previously (Pozzo-Miller et al., 1999a). Membrane ionic currents were recorded using an Axopatch 200B patch-clamp amplifier (Axon Instruments, Foster City, CA), filtered at 2 kHz, digitized at 4 kHz (ITC-16; Instrutech Corporation, Great Neck, NY), and displayed and stored on a PowerMac 9500 computer hard disk (Apple Computer, Cupertino, CA) using custom-written acquisition and analysis software (TIWorkBench, kindly provided by Dr. T. Inoue, Tokyo University, Japan). Typical values of access resistances were <30 MΩ, and whole-cell capacitances were ~100 pF, in all CA1 pyramidal neurons. Cells were discarded for analysis if input resistances measured during hyperpolarizing voltage pulses (−10 mV; 50 msec; every 30 sec) changed by >15% during the course of an experiment. AMPA receptor-mediated miniature EPSCs (mEPSCs) were recorded at a holding membrane potential of −60 mV in the presence of TTX (0.5 μM; Sigma, St. Louis, MO), D,L-APV (100 μM; Research Biochemicals, Natick, MA), and picrotoxin (50 μM; Research Biochemicals). The competitive AMPA receptor antagonist CNQX (20 μM; Research Biochemicals) was used to confirm further that these mEPSCs were indeed mediated by AMPA receptors. The digitized data were analyzed off-line using the Mini-Analysis Program (Synaptosoft, Leonia, NJ) with detection thresholds set at >5 pA and >50 fC for mEPSC amplitude and charge, respectively. Miniature EPSCs were identified and confirmed by analyzing the rise time, decay time, and waveform of each individual spontaneous event.

Quantitative spine density analysis by laser-scanning confocal microscopy. CA1 pyramidal neurons were filled with the fluorescent dye Alexa-594 (absorption at 588 nm, emission at 613 nm; Molecular Probes, Eugene, OR) included in the intracellular patch pipette solution (132 μM). After 15–20 min of whole-cell access and recording, the patch electrode was rapidly removed, and fluorescent images were acquired in the Zeiss Axioskop FS microscope using a monochromator (Polychrome I; TILL Photonics, Planegg, Germany), a rhodamine emission filter, and a cooled CCD frame-transfer camera (PXL-37; Photometrics, Tucson, AZ), all controlled by TIWorkBench, for subsequent identification and correspondence with the mEPSC recordings. The slices were then fixed overnight in 4% paraformaldehyde in PBS at room temperature, mounted and sealed with Vectashield (Vector Laboratories), and imaged using the Olympus LSCM with a 60× (1.2 NA) or a 100× (1.4 NA) oil-immersion lens. In a subset of experiments, slices containing CA1 pyramidal neurons filled with Alexa-594 were further processed for immunostaining of presynaptic terminals using antibodies against synaptobrevin (see Immunocytochemistry and laser-scanning confocal microscopy) and then mounted and imaged in the LSCM. Optical *z*-sections were acquired at 0.5 μm steps through the apical dendritic tree of CA1

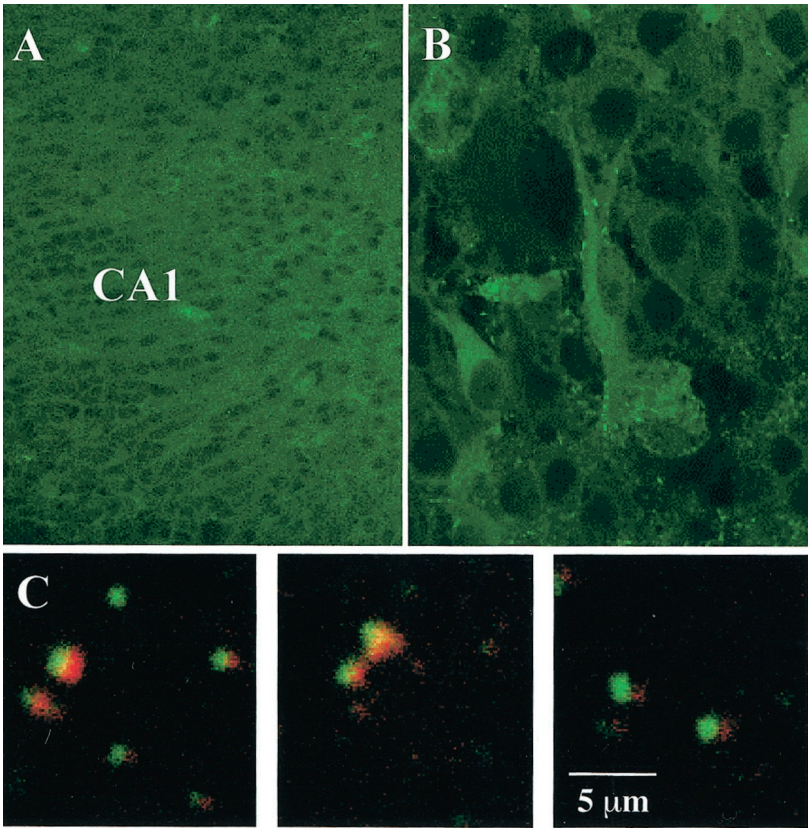

Figure 1. TrkB receptors are expressed at CA1 synapses in organotypic hippocampal slice cultures. *A*, The CA1 region was intensely stained with anti-TrkB antibodies. *B*, The soma and apical dendrites of CA1 pyramidal neurons exhibited TrkB immunoreactivity; punctate staining is shown along the apical dendrites that resembles that of synapses. *C*, Three representative examples of double immunolabeling with anti-TrkB (*green*) and anti-synaptobrevin (*red*) antibodies reveal discrete punctate staining (overlap in *yellow*) in the apical dendritic region of CA1 that resembles that of synaptic junctions.

pyramidal neurons. Dendritic projections with lengths between 1 and 3 μm were identified as spines and counted off-line using NIH Image; care was taken to ensure that each spine was counted only once by following its course through the optical *z*-section reconstruction.

Statistical analysis. All data collection was performed in a blinded manner; the observer making the measurements was not aware of the treatment groups. Data from all the quantitative analyses were analyzed by ANOVA, using Scheffé's *F* procedure for multiple comparisons as the *post hoc* test; $p < 0.05$ was considered statistically significant (StatView; Abacus Concepts, Berkeley, CA). All data shown are presented as the mean ± SEM.

RESULTS

TrkB Receptors are expressed at synapses in organotypic hippocampal slice cultures from postnatal rats

Adult mRNA levels for the TrkB receptor are reached by birth in the rat forebrain, including the hippocampus (Fryer et al., 1996). Confocal immunolabeling was performed to confirm that pyramidal neurons in organotypic hippocampal slice cultures prepared from postnatal day 7 rats and maintained in culture for 2 weeks *in vitro* continue to express TrkB receptors. TrkB immunoreactivity was strongly expressed in all neuronal regions, including the soma and apical dendrites of CA1 pyramidal cells (Fig. 1*A*), with a punctate staining profile that resembled the staining of synapses (Fig. 1*B*). To determine the subcellular synaptic localization of these receptors we performed double immunolabeling of TrkB and synaptobrevin, a synaptic vesicle membrane protein highly enriched in presynaptic terminals. Synaptobrevin (Fig. 1*C*, *red*) and TrkB (Fig. 1*C*, *green*) localized in close apposition in ~80% of the discrete puncta but were rarely completely overlapping (Fig. 1*C*, *yellow*), suggesting that they are present in separate synaptic compartments. We conclude that these puncta indeed represent presynaptic and postsynaptic compartments because the same staining pattern was observed after double immunolabeling of synaptobrevin and CaMKII (an enzyme highly enriched in postsynaptic densities) and double immunolabeling of synaptophysin (another synaptic vesicle protein enriched in preterminals) and CaMKII, whereas double immunolabeling of TrkB and CaMKII was completely overlapping (data not shown). These results suggest that TrkB receptors are localized in postsynaptic dendritic spines, an observation consistent with ultrastructural localization studies (Drake et al., 1999; Aoki et al., 2000). These observations demonstrate that TrkB expression is maintained in organotypic hippocampal slice cultures, including the synaptic localization, allowing us to investigate further the effects of BDNF on synaptic vesicle distribution and excitatory synaptic transmission in this model system.

BDNF increases the number of docked vesicles at the active zone of excitatory synapses onto CA1 pyramidal neurons

Knock-out mice lacking the *bdnf* gene exhibit exacerbated synaptic depression during high-frequency stimuli, fewer docked vesicles, and reduced expression levels of synaptobrevin and synaptophysin than their wild-type littermates (Pozzo-Miller et al., 1999b). Furthermore, *trkB* knock-out mice also have a decreased density of synaptic vesicles in hippocampal synapses (Martínez et al., 1998). If BDNF–TrkB signaling is necessary for competent synaptic vesicle docking at active zones, exogenous application of BDNF to normal rat hippocampal slices should modulate synaptic vesicle distribution within presynaptic terminals. To test this hypothesis we performed quantitative electron microscopy on excitatory asymmetric synapses on CA1 dendritic spines. The distribution of synaptic vesicles within presynaptic terminals was measured in two distinct and mutually exclusive

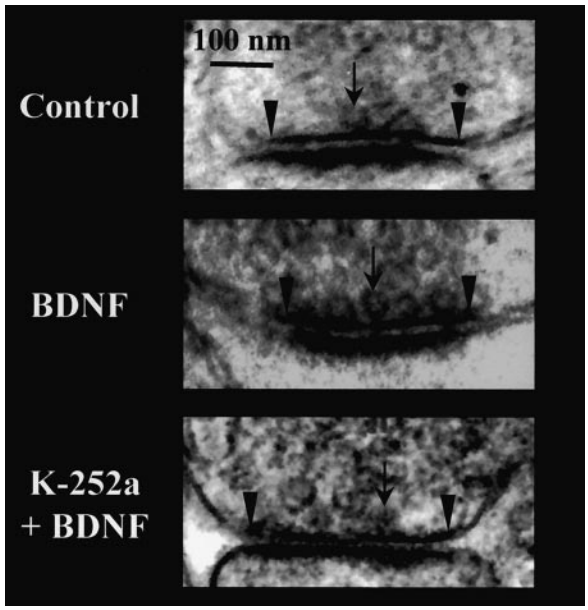

Figure 2. Representative electron micrographs of synapses on dendritic spines within CA1 stratum radiatum from control (*top*), BDNF-treated (*middle*), and K-252a + BDNF-treated (*bottom*) slice cultures. Reserve pool vesicles, docked vesicles (*arrows*), and the boundaries of the active zone (*arrowheads*) are shown.

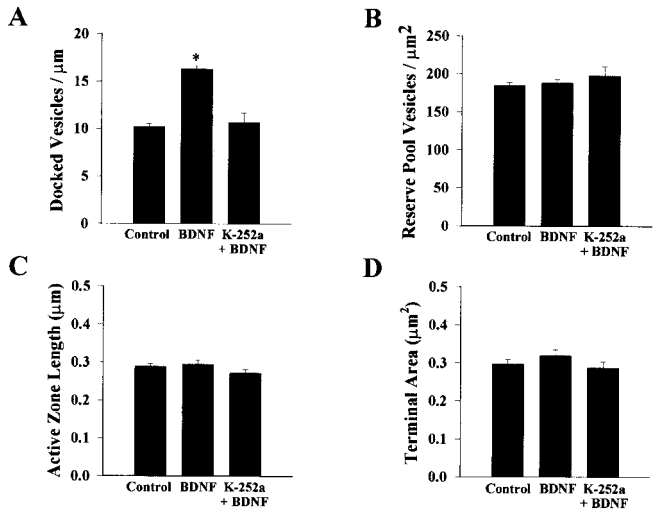

Figure 3. BDNF increases the number of docked vesicles at excitatory CA1 spine synapses, without affecting reserve pool vesicles. *A*, Histogram plot of the number of docked synaptic vesicles per micrometer of active zone. *B*, Histogram plot representing the number of reserve pool vesicles per square micrometer of presynaptic terminal. *C*, Histogram plot of the active zone length. *D*, Histogram plot of the area of the presynaptic terminal. Data in all *panels* are means ± SEM (control, $n = 98$ synapses; BDNF, $n = 101$ synapses; K-252a + BDNF, $n = 53$ synapses; an *asterisk* indicates $p < 0.05$).

domains: (1) docked vesicles were counted if they were in close apposition (~50 nm) to the presynaptic active zone (Fig. 2), and (2) reserve pool vesicles were defined as those synaptic vesicles within the perimeter of the synaptic terminal region but outside of the docked vesicle region. To avoid the bias of selecting the larger synapses in single thin sections, only those synapses with presynaptic terminals and active zones of similar magnitude were included in the analysis; a total of 293 synapses from eight slices fit the above criteria and were included in the statistical analysis (control, $n = 98$; BDNF, $n = 101$; K-252a + BDNF, $n = 53$; and K-252a, $n = 41$; two slices in each group). In those sampling groups there were no differences in the presynaptic terminal area (0.3 ± 0.01, 0.32 ± 0.02, 0.29 ± 0.02, and 0.3 ± 0.02 μm^2, for control, BDNF, K-252a + BDNF, and K-252a, respectively; ANOVA, Scheffé's *F post hoc*, $p > 0.05$) or the active zone length (0.29 ± 0.01, 0.29 ± 0.01, 0.27 ± 0.01, and 0.27 ± 0.01 μm, for control, BDNF, K-252a + BDNF, and K-252a, respectively; $p > 0.05$). To assess directly the effects of BDNF and because of the unknown content of trophic factors in the horse serum-containing media, all of the treatments in the following experiments were performed in serum-free media.

Application of BDNF (250 ng/ml in serum-free media) to hippocampal slice cultures for 5–9 div significantly increased the number of docked vesicles (DV) at the active zone from 10.21 ± 0.34 DV/μm of active zone to 16.29 ± 0.35 DV/μm ($p < 0.0001$ compared with serum-free controls; Fig. 3*A*). This effect of BDNF was blocked by cotreatment with K-252a (10.66 ± 1.01 DV/μm; $p < 0.0001$ compared with BDNF; Fig. 3*A*), a compound that, at the concentration used (200 nM), specifically inhibits the autophosphorylation of tyrosine kinase domains of plasma membrane neurotrophin receptors, not affecting soluble tyrosine kinases (Tapley et al., 1992). Treatment with K-252a (200 nM) alone in serum-free media did not affect the number of docked vesicles (9.24 ± 0.52; $p > 0.05$ compared with control; data not shown). On the other hand, there were no differences in the number of reserve pool vesicles (RP) across all groups (control, 185 ± 3.9 RP/μm^2 of terminal; BDNF, 188 ± 5.1 RP/μm^2; K-252a + BDNF, 198 ± 12.9 RP/μm^2; and K-252a, 186 ± 3.8 RP/μm^2; $p > 0.05$; Fig. 3*B*). We estimated that BDNF increased the total number of docked vesicles per active zone from 8.9 to 21.8 docked vesicles (see Materials and Methods).

We subsequently addressed the possibility that BDNF treatment may affect synapse size and thereby active zone length and docked vesicle numbers, although in the previous experiment the number of docked vesicles was normalized by micrometer of active zone length and the sampling was unbiased to synaptic size by selecting synapses of similar magnitude for the statistical comparisons between all groups. The length of the active zone measured in asymmetric spine synapses observed in a random sample of neuropil fields within CA1 stratum radiatum (Fig. 4*A*) was slightly, although significantly, larger in BDNF-treated slices (0.237 ± 0.007 vs 0.264 ± 0.007 μm; $p = 0.01$; Fig. 4*B*). Because active zones were only ~11% larger in BDNF-treated slices and the number of DV per micrometer was ~60% larger in those slices, these results suggest that BDNF most likely increases the packing density of docked vesicles at the active zone, with minor effects on synapse size. In fact, three-dimensional reconstructions indicate that the relationship between active zone size and the number of docked vesicles is approximately linear in CA1 synapses, with docked vesicles occupying only ~60% of the active zone (Schikorski and Stevens, 1997), suggesting that the packing density of vesicles can be increased. Our results directly demonstrate that BDNF modulates synaptic vesicle distribution within presynaptic terminals in CA1 excitatory spine synapses of hippocampal slices by increasing the number of docked vesicles at the active zone.

BDNF increases the frequency of AMPA-mediated mEPSCs without affecting their amplitude

It has been repeatedly proposed that synaptic vesicles docked at the active zone are the morphological correlate of the physiolog-

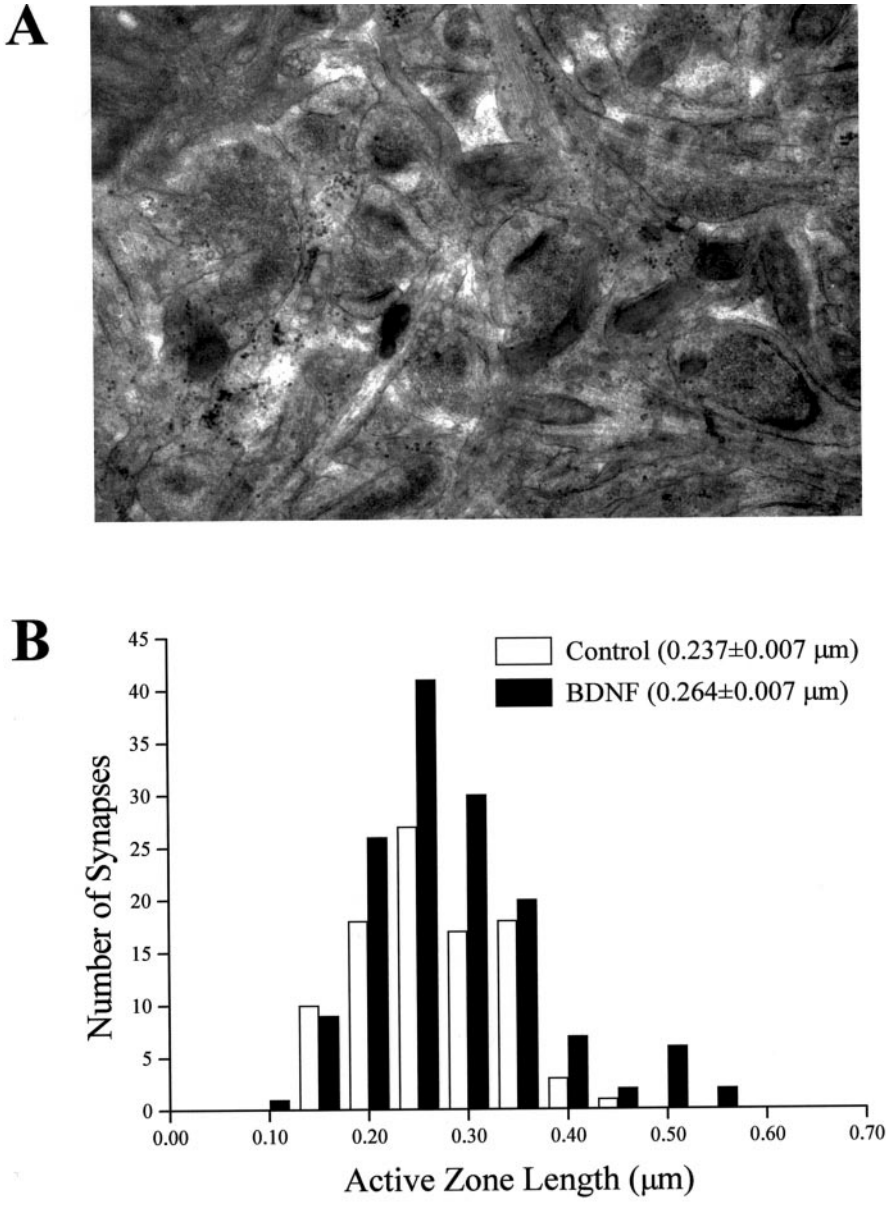

Figure 4. The length of the active zone in CA1 asymmetric spine synapses is slightly larger in BDNF-treated slice cultures. *A*, Representative electron micrograph showing a neuropil field (24 μm^2) within CA1 stratum radiatum (from a BDNF-treated slice in this example) that was used for random sampling of synapses. *B*, Frequency histogram distributions of the active zone length of randomly sampled CA1 spine synapses in 50 nm bins. The distribution of active zone lengths is slightly skewed toward the larger size bins in the BDNF-treated slices. Note also that the BDNF-treated group has a higher number of synapses in the same sampling area (see Results).

ically defined readily releasable quantal pool (Harris and Sultan, 1995; Stevens and Tsujimoto, 1995; von Gersdorff et al., 1996; Zucker, 1996; Dobrunz and Stevens, 1997; Murthy et al., 1997; Ryan et al., 1997; Schikorski and Stevens, 1997; Pyle et al., 2000; Stevens and Williams, 2000; Südhof, 2000). However, a manipulation that increases the number of docked vesicles while enhancing quantal neurotransmitter release is necessary to demonstrate directly such a correspondence. The observation that BDNF increases the number of docked vesicles at the active zone predicts an enhancement in mEPSC frequency, thus providing the manipulation required to demonstrate the correspondence between docked vesicles and readily releasable quanta. Whole-cell recordings were performed in CA1 pyramidal neurons in the presence of TTX (0.5 μM) to investigate the consequences of increasing the number of docked vesicles on quantal transmitter release. AMPA receptor-mediated mEPSCs (Fig. 5*A*) were recorded at a holding potential of −60 mV in the presence of D,L-APV (100 μM) and picrotoxin (50 μM) to block NMDA and $GABA_A$ receptors, respectively; further addition of the AMPA receptor antagonist CNQX (20 μM) completely abolished all postsynaptic currents (data not shown). Typical continuous records of membrane ionic current showing spontaneous mEPSCs are illustrated in Figure 5*B*.

BDNF increased the frequency of mEPSCs recorded from CA1 pyramidal neurons from 1.34 ± 0.24 Hz (six cells from three slices) in serum-free controls to 3.81 ± 0.61 Hz (six cells from three slices; $p = 0.0027$; Fig. 5*B*), an effect clearly illustrated in the cumulative frequency distributions (Fig. 6*A*). This effect of BDNF was blocked by incubation with K-252a (2.13 ± 0.35 Hz; seven cells from three slices; $p = 0.0426$ compared with BDNF; Fig. 5*B*). Treatment with K-252a alone in serum-free media did not significantly affect mEPSC frequency (0.648 ± 0.227 Hz; $p = 0.6798$ compared with control; data not shown). Despite this pronounced enhancement of mEPSC frequency in BDNF-treated slices, there were no differences in the mean amplitude of mEPSCs across all groups (control, 26.61 ± 2.14 pA; BDNF, 24.50 ± 2.43 pA; K-252a + BDNF, 29.99 ± 1.90 pA; and K-252a, 26.99 ± 4.35 pA; $p > 0.05$); in fact, the cumulative amplitude distributions

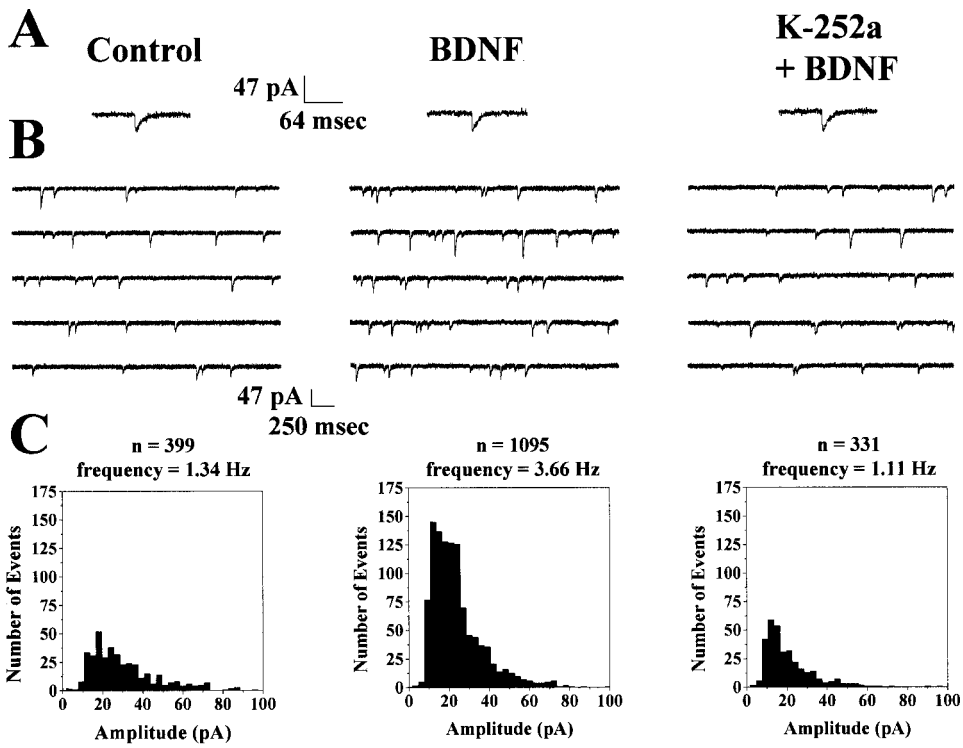

Figure 5. BDNF increases the frequency of AMPA-mediated mEPSCs without affecting their amplitude. Data are from one control (*left*), one BDNF-treated (*middle*), and one K-252a + BDNF-treated (*right*) neuron. *A*, Representative AMPA-mediated mEPSCs. BDNF (*middle*) or K-252a + BDNF (*right*) did not effect the kinetics or amplitude of AMPA mEPSCs. *B*, Representative continuous records of membrane currents showing AMPA mEPSC events from control (*left*), BDNF-treated (*middle*), and K-252a + BDNF-treated (*right*) slice cultures. *C*, Frequency histogram distributions for each of the three depicted cells in 5 pA bins. The total number of events and the frequency of mEPSCs are shown above the frequency histogram distributions.

are nearly superimposed (Fig. 6*B*). Furthermore, the kinetics of individual mEPSCs was not statistically different across all treatment groups (rise times for control, 5.07 ± 0.39 msec; BDNF, 4.97 ± 0.30 msec; K-252a + BDNF, 5.4 ± 0.12 msec; and K-252a, 5.24 ± 0.49 msec; $p > 0.05$; decay times for control, 12.05 ± 0.74 msec; BDNF, 10.92 ± 1.03 msec; K-252a + BDNF, 12.7 ± 0.27 msec; and K-252a, 9.38 ± 1.29 msec; $p > 0.05$). Thus, the increase in mEPSC frequency was not accompanied by a change in the sensitivity of the postsynaptic cell to the synaptically released neurotransmitter, indicated by the lack of change in the mEPSC amplitude distributions or in the kinetics of the individual quantal events. Together with the effect of BDNF on synaptic vesicle distribution, these results demonstrate that BDNF enhances excitatory synaptic transmission at CA1 synapses in hippocampal slices via at least a presynaptic mechanism.

BDNF increases the number of synapses per neuron

The aforementioned observations support our hypothesis that BDNF enhances quantal neurotransmitter release by increasing the number of vesicles docked at the active zone of individual synapses. An additional contributing factor for the observed higher mEPSC frequency is that CA1 pyramidal neurons in BDNF-treated slices receive more synaptic input by having a higher synaptic density. Indeed, BDNF–TrkB signaling has been shown to enhance dendritic growth and branching (McAllister et al., 1995), as well as spine dynamics (Horch et al., 1999) in slice cultures from ferret visual cortex. BDNF has also been shown to increase dendritic spine density in cerebellar Purkinje neurons in culture (Shimada et al., 1998). To account for the potential role of higher synaptic input on the observed increase in mEPSC frequency, we estimated synaptic density using two independent methods: (1) directly counting asymmetric spine synapses in random fields of CA1 stratum radiatum sampled by electron microscopy and (2) measuring the spine density in the apical dendrites of individual CA1 pyramidal neurons by confocal microscopy.

Spine density was measured by confocal microscopy of individual CA1 pyramidal neurons filled with the fluorescent dye Alexa-594 via the patch pipette during whole-cell recording of mEPSCs (see Fig. 8*A,B*). Dendritic spine counts were performed in a total apical dendritic length of 1674 μm in control slices (five cells from four slices), 1269 μm in BDNF-treated slices (five cells from four slices), 1454 μm in K-252a + BDNF-treated slices (seven cells from two slices), and 644 μm in K-252a-treated slices (eight cells from three slices); all data were normalized per 10 μm of dendritic length. To confirm that these spines indeed represent actual synapses, immunolabeling of synaptobrevin (Fig. 7*A*, *green*) was performed in slices containing Alexa-filled CA1 pyramidal cells [Fig. 7*A*, *red* (*yellow* represents overlap)]. Dendritic spines from cells filled with Alexa-594 dye were in close apposition to clearly identifiable presynaptic terminals labeled with synaptobrevin (Fig. 7*B*) in ~65% of the cases (465 μm of apical dendritic length; four cells from three serum-free control slices; Fig. 7*C*). This number represents a lower limit of the proportion of spines with preterminal partners, because the identification of both Alexa-filled spines and synaptobrevin-immunoreactive puncta is limited by the spatial resolution of the confocal microscope, as well as by the detection sensitivity of the immunocytochemical reaction.

CA1 pyramidal neurons had an increased apical dendrite spine density in BDNF-treated slices (5.6 ± 0.2 spines/10 μm, five cells from four slices, vs 10.6 ± 0.2 spines/10 μm, five cells from four slices; $p < 0.0001$; Fig. 8*C*). Inhibition of TrkB receptor activation with K-252a not only blocked the effect of BDNF but further reduced spine density compared with controls (2.8 ± 0.1 spines/10 μm; seven cells from two slices; $p < 0.0001$ compared with BDNF; Fig. 8*C*). Treatment with K-252a alone in serum-free medium had a similar effect on spine density (2.9 ± 0.2 spines/10 μm; eight cells from three slices; $p < 0.0001$ compared with controls; data not shown). These results were confirmed using the BDNF scavenger TrkB-IgG [20 μg/ml in the presence of BDNF (Shelton et al., 1995)]; CA1 pyramidal neurons had fewer spines

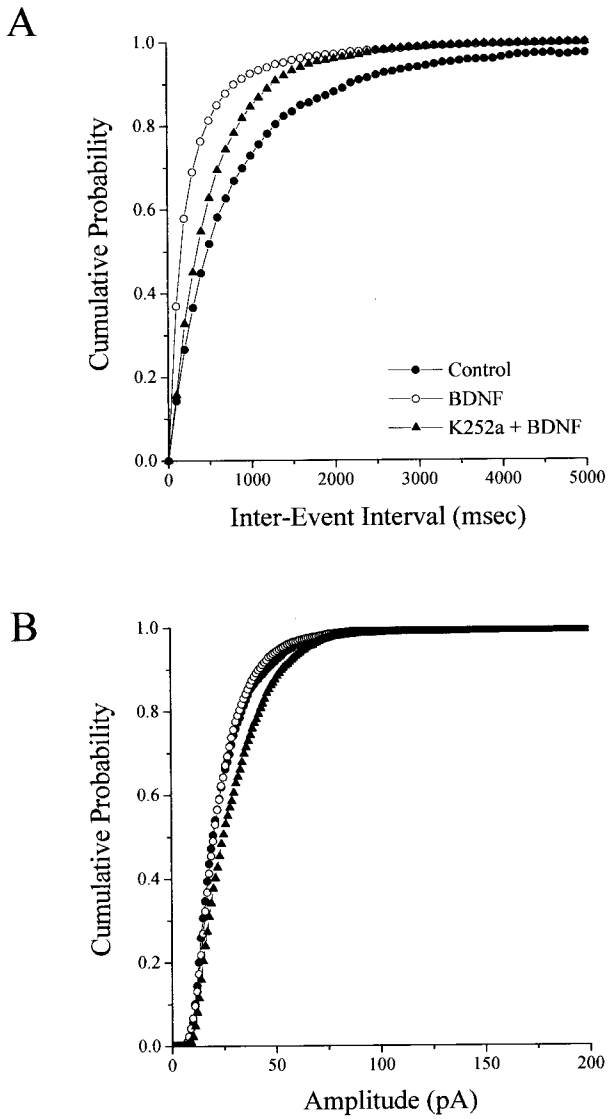

Figure 6. BDNF increases the frequency but not the amplitude of AMPA mEPSCs. *A*, Cumulative probability distribution of inter-event (mEPSC) interval in all neurons analyzed (6 cells in control, *filled circles*; 6 cells in BDNF-treated slices, *open circles*; and 7 cells in K-252a + BDNF-treated slices, *filled triangles*). *B*, Cumulative probability distribution of mEPSC amplitude in all neurons analyzed (6 cells in control, *filled circles*; 6 cells in BDNF-treated slices, *open circles*; and 7 cells in K-252a + BDNF-treated slices, *filled triangles*). Note that the difference between the K-252a + BDNF-treated set and the other two groups is not statistically significant at $p < 0.05$ (see Results). Error bars have been removed for clarity.

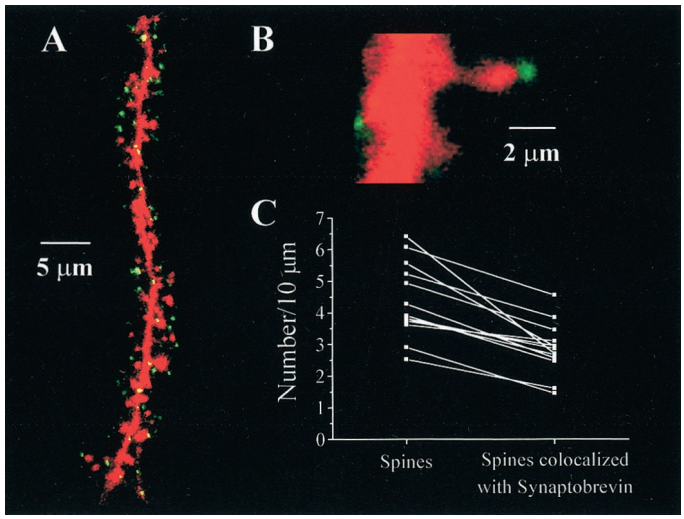

Figure 7. Most CA1 pyramidal neuron dendritic spines have presynaptic partners. *A*, Confocal microscopy image of a representative segment of the apical dendrite of a CA1 pyramidal neuron filled with Alexa-594 (*red*) via the patch electrode during whole-cell recording in a control slice subsequently processed for synaptobrevin immunoreactivity (*green*). Note that most dendritic spines colocalize with synaptobrevin-positive puncta [*yellow* (overlap)]. *B*, Higher magnification view of an Alexa-filled spine with a synaptobrevin-positive presynaptic terminal. *C*, Scatterplot of the number of spines identified solely by Alexa-filling (*left*) and the number of synapses identified by Alexa-filling and subsequent immunolabeling of presynaptic terminals with anti-synaptobrevin antibodies (*right*). The numbers of spines and synapses (normalized per 10 μm of apical dendrite) in each analyzed segment are connected by *lines* to show the proportion of spines with presynaptic partners (~65%).

in slice cultures treated with TrkB-IgG (4.7 ± 0.12 spines/10 μm; four cells from two slices; $p < 0.0001$ compared with BDNF; data not shown).

The aforementioned results were confirmed by electron microscopy counts of asymmetric spine synapses in a random sample of neuropil fields within CA1 stratum radiatum (Fig. 4*A*; individual sampling area, 24 μm^2; total sampling area, 680 μm^2); BDNF-treated slices had a higher synaptic density compared with serum-free controls (5.14 ± 0.3 synapses/24 μm^2 of neuropil vs 3.29 ± 0.34 synapses/24 μm^2; $p = 0.0002$; data not shown). Thus, a higher spine density and therefore an increase in the number of excitatory synapses may also contribute to the increased mEPSC frequency by augmenting the synaptic input to CA1 neurons. Despite the fact that spine density was lower in both K-252a-treated groups (in the presence and absence of BDNF) compared with controls, the mEPSC frequency in those K-252a groups was similar to that in control slices, indicating that CA1 neurons may receive a comparable amount of synaptic input (reflected in the mEPSC frequency) although they have a significantly lower synaptic density. This argument suggests that the major effect of BDNF on quantal neurotransmitter release is presynaptic, most likely by increasing the number of docked vesicles at active zones of excitatory spine synapses.

DISCUSSION

We present evidence that BDNF modulates presynaptic properties of excitatory spine synapses on CA1 pyramidal neurons in hippocampal slices via a plasma membrane tyrosine kinase-dependent mechanism. BDNF increased the number of synaptic vesicles docked at the active zone and increased the frequency of AMPA receptor-mediated mEPSCs, without affecting their mean amplitude or rise or decay times. The increase in spine and synapse density suggests that BDNF has also postsynaptic effects that may partly contribute to the effects observed on quantal neurotransmitter release. These results provide insights into some of the mechanisms by which BDNF modulates hippocampal synaptic physiology and plasticity.

Modulation of the readily releasable pool (RRP) of synaptic vesicles has received considerable attention recently as a mechanism for the regulation of synaptic strength. The observation that BDNF increases both the frequency of mEPSCs and the packing density of docked vesicles reinforces the hypothesis that those vesicles correspond to the RRP of quanta (Harris and Sultan,

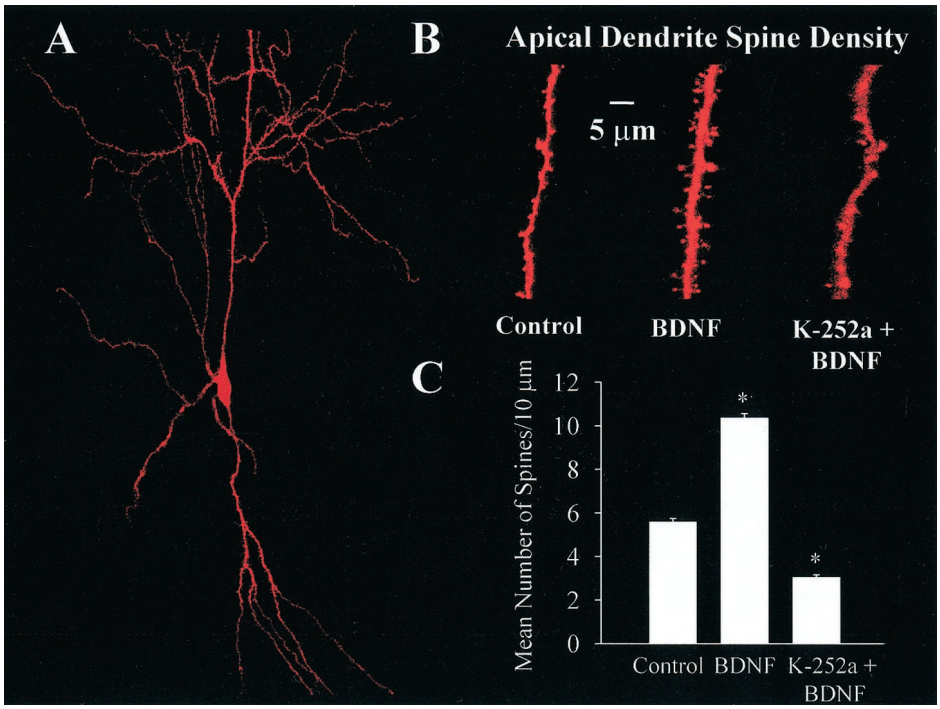

Figure 8. BDNF increases spine density in CA1 pyramidal neurons. *A*, Representative CA1 pyramidal neuron from a BDNF-treated slice filled with Alexa-594 and imaged by confocal microscopy. *B*, Higher magnification views of representative segments of apical dendrites from control (*left*), BDNF-treated (*middle*), and K-252a + BDNF-treated (*right*) slices used to quantify dendritic spine density. *C*, Histograms of the number of dendritic spines per 10 μm of CA1 pyramidal neuron apical dendrite. An *asterisk* indicates $p < 0.05$.

1995; Stevens and Tsujimoto, 1995; von Gersdorff et al., 1996; Zucker, 1996; Dobrunz and Stevens, 1997; Murthy et al., 1997; Ryan et al., 1997; Schikorski and Stevens, 1997; Pyle et al., 2000; Stevens and Williams, 2000; Südhof, 2000). Increasing the size of this RRP would allow synapses to sustain longer epochs or higher frequencies of transmitter release before depletion (Dobrunz and Stevens, 1997; Murthy et al., 1997). These observations support the hypothesis that BDNF facilitates the induction of LTP by allowing synapses to follow high-frequency afferent activity (Figurov et al., 1996; Gottschalk et al., 1998; Pozzo-Miller et al., 1999b). The only manipulation that increases the physiologically defined RRP described to date is phorbol ester activation of protein kinase C (PKC) (Stevens and Sullivan, 1998; Waters and Smith, 2000). Interestingly, TrkB receptor activation by BDNF can lead to PKC activation via the phospholipase Cγ-1–diacylglycerol signaling pathway (Segal and Greenberg, 1996). BDNF also enhances glutamate release from synaptosomes by mitogen-activated protein kinase-dependent phosphorylation of synapsin-I, an effect not observed in synapsin-I and/or -II knockout mice (Jovanovic et al., 2000). Because one of the major functions of synapsins is to regulate the trafficking of synaptic vesicles between distinct pools within presynaptic terminals (Greengard et al., 1993), it seems likely that BDNF facilitates synaptic vesicle docking via the modulation of presynaptic vesicle proteins (Pozzo-Miller et al., 1999b).

It has been proposed that the release probability of evoked EPSCs at single synapses is linearly related to the size of the RRP (Dobrunz and Stevens, 1997; Murthy et al., 1997) and therefore proportional to the number of docked vesicles (Harris and Sultan, 1995; Schikorski and Stevens, 1997). Because it has been shown that the size of the active zone and the number of docked vesicles are directly correlated (Harris and Sultan, 1995; Schikorski and Stevens, 1997), sampling a homogenous population of synapses eliminates any sampling biases of synapse size on differences that may be observed in synaptic vesicle distributions. It was thus crucial in our study that synaptic terminals of similar magnitudes were chosen for statistical analysis. Furthermore, estimating TDV from single two-dimensional sections yields results in agreement with actual counts of docked vesicles obtained from a complete three-dimensional reconstruction of presynaptic active zones [10.3 ± 5.6 and 4.6 ± 3.0 docked vesicles per active zone in the adult mouse hippocampal CA1 region and primary cultures of embryonic hippocampal neurons, respectively; from Schikorski and Stevens (1997)]. It is expected that the distributions estimated in hippocampal organotypic slice cultures (8.9 docked vesicles in controls) fall between the ones observed in brain and primary cultures; thus, organotypic cultures provide a representative model of hippocampal synapses to study synaptic vesicle distributions.

The issue of how BDNF enhances glutamatergic synaptic transmission, presynaptically or postsynaptically, remains highly controversial. The frequency of mEPSCs depends on the probability of release from presynaptic terminals (Fatt and Katz, 1952), whereas mEPSC amplitude is dependent on several factors, including, but not limited to, the amount of transmitter released, the postsynaptic sensitivity, and the driving force for the ions mediating the synaptic current (Van der Kloot, 1991). It was originally shown in primary hippocampal cultures that BDNF increased the amplitude of spontaneous action potential-dependent EPSCs, as well as of glutamate- and NMDA-evoked currents, via postsynaptic tyrosine kinase activation (Levine et al., 1995). In contrast, other groups have reported in the same preparation that BDNF increased the frequency of mEPSCs, without affecting mEPSC amplitude or the amplitude of glutamate-evoked currents (Li et al., 1998a), but only when functional TrkB receptors are expressed in the presynaptic neuron in paired recordings (Li et al., 1998b). Furthermore, BDNF decreased both paired-pulse facilitation and the coefficient of variation of evoked EPSCs (Lessman and Heumann, 1998; Berninger et al., 1999; Schinder et al., 2000), two robust indicators of presynaptic properties, such as release probability and the number of release sites. The results presented here demonstrate that

BDNF increases the frequency without affecting the properties of individual quantal events in postnatal hippocampal slice cultures, a preparation that retains more intrinsic hippocampal circuitry than do primary cultures of dissociated embryonic neurons. We cannot exclude, however, other postsynaptic effects of BDNF (Levine et al., 1998), such as enhanced Ca^{2+} entry via NMDA receptors or voltage-dependent calcium channels or Ca^{2+} release from intracellular stores (Pozzo-Miller et al., 2000).

To date, most reports focused on acute (seconds to minutes) actions of BDNF on embryonic hippocampal neurons in culture, whereas few studies have addressed issues regarding long-term actions of BDNF. However, high-level expression and certain levels of constitutive secretion of neurotrophic factors suggest that long-term neurotrophic regulation of synaptic transmission may be a physiological form of neurotrophin action. Chronic application of BDNF to hippocampal or cortical neurons in dissociated cultures results in complex effects on synaptic transmission, including activity-dependent scaling of the quantal amplitude of AMPA-mediated synaptic currents (Rutherford et al., 1998), increases in quantal amplitude of autaptic currents (Sherwood and Lo, 1999), and an increase in mEPSC frequency without a concomitant increase of synaptic profiles (Vicario-Abejon et al., 1998). A recent study reported increases in both the frequency and amplitude of AMPA receptor-mediated mEPSCs after 4–7 d of BDNF incubation (Bolton et al., 2000); this apparent discrepancy with the lack of effect on AMPA mEPSC amplitude observed here may originate from the fact that BDNF was applied in serum-containing media. In this context, we interpret that serum starvation seems to contribute to spine loss in our slice cultures and that BDNF provides a "missing," but necessary, factor for spine maintenance. CA1 neuron spine density in slice cultures maintained in the presence of serum is ~1 spine/μm (Pozzo-Miller et al., 1999a), comparable with the spine density of slice cultures treated with BDNF in the absence of serum, whereas serum-starved slices have ~53% fewer spines. Furthermore, preliminary measurements in CA1 cells in slices treated with BDNF in the presence of serum yielded no effects on spine density (L. D. Pozzo-Miller, unpublished observations). It seems that a reduction in spontaneous mEPSC activity may eventually lead to complete spine loss, because spine maintenance in slice cultures requires ongoing AMPA receptor-mediated mEPSCs (McKinney et al., 1999).

Our observation of an increase in the frequency of mEPSCs could be partly caused by an increase in the synaptic input to the neurons. We observed an ~180% increase in the frequency of AMPA mEPSCs but only an ~60% increase in the number of docked vesicles after long-term BDNF treatment. Consistently, BDNF increased dendritic spine and synaptic density by ~90 and ~57%, respectively, suggesting that this increase in synaptic density contributed partially to the enhanced mEPSC frequency. Hippocampal neurons reversibly shed their dendritic spines after experimental deafferentation, making the spine density a good indicator of synaptic density (Parnavelas et al., 1974). Furthermore, immunolabeling of synaptobrevin in slices with Alexa-filled CA1 neurons revealed that at least ~65% of spines in hippocampal slice cultures have presynaptic terminals, as suggested previously (Pozzo-Miller et al., 1999a). The observation that CA1 neurons in both K-252a-treated groups (in the presence and absence of BDNF) had fewer spines than did control cells but exhibited mEPSC frequencies similar to those of control neurons suggests that the major site of action of BDNF on spontaneous quantal transmitter release is indeed presynaptic. Because spine maintenance requires spontaneous AMPA mEPSCs (McKinney et al., 1999), the observed increase in spine density may result from the higher mEPSC frequency in BDNF-treated slices. Alternatively, BDNF may directly increase dendritic branching (McAllister et al., 1995) as well as promote the formation of functional excitatory synapses (Shimada et al., 1998; Vicario-Abejon et al., 1998) by a direct postsynaptic mechanism(s). Together with the postsynaptic localization of TrkB receptors (Drake et al., 1999; Aoki et al., 2000), these observations suggest that the presynaptic effects are mediated by a retrograde messenger(s).

Deciphering the mechanisms underlying the actions of BDNF on hippocampal synaptic transmission is essential in making progress toward our understanding of the interplay between hippocampal synaptic plasticity and learning and memory processes. Because it appears that BDNF enhances synaptic transmission in accordance with Katz's quantal hypothesis, BDNF should be considered a valuable tool for investigating not only hippocampal synaptic plasticity but also fundamental and long-standing issues regarding central synaptic physiology in the CNS.

REFERENCES

Aoki C, Wu K, Elste A, Len GW, Lin SY, McAuliffe G, Black IB (2000) Localization of brain-derived neurotrophic factor and TrkB receptors to postsynaptic densities of adult rat cerebral cortex. J Neurosci Res 59:454–463.

Berninger B, Schinder AF, Poo M-m (1999) Synaptic reliability correlates with reduced susceptibility to synaptic potentiation by brain-derived neurotrophic factor. Learn Mem 6:232–242.

Bliss TVP, Collingridge GL (1993) A synaptic model of memory: long-term potentiation in the hippocampus. Nature 361:31–39.

Bolton MM, Pittman AJ, Lo DC (2000) Brain-derived neurotrophic factor differentially regulates excitatory and inhibitory synaptic transmission in hippocampal cultures. J Neurosci 20:3221–3232.

Dickinson-Nelson A, Reese TS (1983) Structural changes during transmitter release at synapses in the frog sympathetic ganglion. J Neurosci 3:42–52.

Dobrunz LE, Stevens CF (1997) Heterogeneity of release probability, facilitation, and depletion at central synapses. Neuron 18:995–1008.

Drake CT, Milner TA, Patterson SL (1999) Ultrastructural localization of full-length trkB immunoreactivity in rat hippocampus suggests multiple roles in modulating activity-dependent synaptic plasticity. J Neurosci 19:8009–8026.

Fatt P, Katz B (1952) Spontaneous subthreshold activity at motor nerve endings. J Physiol (Lond) 117:109–128.

Figurov A, Pozzo-Miller LD, Olafsson P, Wang T, Lu B (1996) Regulation of synaptic responses to high-frequency stimulation and LTP by neurotrophins in the hippocampus. Nature 381:706–709.

Fryer RH, Kaplan DR, Feinstein SC, Radeke MJ, Grayson DR, Kromer LF (1996) Developmental and mature expression of full-length and truncated TrkB receptors in the rat forebrain. J Comp Neurol 374:21–40.

Gottschalk W, Pozzo-Miller LD, Figurov A, Lu B (1998) Presynaptic modulation of synaptic transmission and plasticity by brain-derived neurotrophic factor in the developing hippocampus. J Neurosci 18:6830–6839.

Greengard P, Valtorta F, Czernik AJ, Benfenati F (1993) Synaptic vesicle phosphoproteins and regulation of synaptic function. Science 259:780–785.

Harris KM, Sultan P (1995) Variation in the number, location and size of synaptic vesicles provides an anatomical basis for the nonuniform probability of release at hippocampal CA1 synapses. Neuropharmacology 34:1387–1395.

Heuser JE, Reese TS (1973) Evidence for recycling of synaptic vesicle membrane during transmitter release at the frog neuromuscular junction. J Cell Biol 57:315–344.

Horch HW, Kruttgen A, Protbury SD, Katz LC (1999) Destabilization of cortical dendrites and spines by BDNF. Neuron 23:353–364.

Jensen FE, Harris KM (1989) Preservation of neuronal ultrastructure in hippocampal slices using rapid microwave-enhanced fixation. J Neurosci Methods 29:217–230.

Jovanovic JN, Czernik AJ, Fiennberg AA, Greengard P, Sihra TS (2000) Synapsins as mediators of BDNF-enhanced neurotransmitter release. Nat Neurosci 3:323–329.

Katz B (1969) The release of neural transmitter substances. Liverpool, England: Liverpool University.

Korte M, Carroll P, Wolf E, Brem G, Thoenen H, Bonhoeffer T (1995)

Hippocampal long-term potentiation is impaired in mice lacking brain-derived neurotrophic factor. Proc Natl Acad Sci USA 92:8856–8860.
Lessman V, Heumann R (1998) Modulation of unitary glutamatergic synapses by neurotrophin-4/5 or brain-derived neurotrophic factor in hippocampal microcultures: presynaptic enhancement depends on pre-established paired-pulse facilitation. Neuroscience 86:399–413.
Lessman V, Gottmann K, Heumann R (1994) BDNF and NT-4/5 enhance glutamatergic synaptic transmission in cultured hippocampal neurons. NeuroReport 6:21–25.
Levine ES, Dreyfus CF, Black IB, Plummer MR (1995) Brain-derived neurotrophic factor rapidly enhances synaptic transmission in hippocampal neurons via postsynaptic tyrosine kinase receptors. Proc Natl Acad Sci USA 92:8074–8077.
Levine ES, Crozier RA, Black IB, Plummer MR (1998) Brain-derived neurotrophic factor modulates hippocampal synaptic transmission by increasing *N*-methyl-D-aspartic acid receptor activity. Proc Natl Acad Sci USA 95:10235–10239.
Lewin GR, Barde Y (1996) Physiology of the neurotrophins. Annu Rev Neurosci 19:289–317.
Li YX, Zhang Y, Lester HA, Schuman EM, Davidson N (1998a) Enhancement of neurotransmitter release induced by brain-derived neurotrophic factor in cultured hippocampal neurons. J Neurosci 18:10231–10240.
Li YX, Xu Y, Ju D, Lester HA, Davidson N, Schuman EM (1998b) Expression of a dominant negative TrkB receptor, T1, reveals a requirement for presynaptic signaling in BDNF-induced synaptic potentiation in cultured hippocampal neurons. Proc Natl Acad Sci USA 95:10884–10889.
Martínez A, Alcántara S, Borrell V, Del Río JA, Blasi J, Otal R, Campos N, Boronat A, Barbacid M, Silos-Santiago I, Soriano E (1998) TrkB and TrkC signaling are required for maturation and synaptogenesis of hippocampal connections. J Neurosci 18:7336–7350.
McAllister AK, Lo DC, Katz LC (1995) Neurotrophins regulate dendritic growth in developing visual cortex. Neuron 15:791–803.
McAllister AK, Katz LC, Lo DC (1999) Neurotrophins and synaptic plasticity. Annu Rev Neurosci 22:295–318.
McKinney RA, Capogna M, Durr R, Gähwiler BH, Thompson SM (1999) Miniature synaptic events maintain dendritic spines via AMPA receptor activation. Nat Neurosci 2:44–49.
Minichiello L, Korte M, Wolfer D, Kuhn R, Unsicker K, Cestari V, Rossi-Arnaud C, Lipp HP, Bonhoeffer T, Klein R (1999) Essential role for TrkB receptors in hippocampus-mediated learning. Neuron 24:401–414.
Model PG, Highstein SM, Bennett MV (1975) Depletion of vesicles and fatigue of transmission at a vertebrate central synapse. Brain Res 98:209–228.
Murthy VN, Sejnowski TJ, Stevens CF (1997) Heterogeneous release properties of visualized individual hippocampal synapses. Neuron 18:599–612.
Parnavelas JG, Lynch G, Brecha N, Cotman CW, Globus A (1974) Spine loss and regrowth in hippocampus following deafferentation. Nature 248:71–73.
Patterson SL, Abel T, Deuel TAS, Martin KC, Rose JC, Kandel ER (1996) Recombinant BDNF rescues deficits in basal synaptic transmission and hippocampal LTP in BDNF Knockout mice. Neuron 16:1137–1145.
Pozzo-Miller LD, Petrozzino JJ, Mahanty NK, Connor JA (1993) Optical imaging of cytosolic calcium, electrophysiology, and ultrastructure in pyramidal neurons of organotypic slice cultures from rat hippocampus. NeuroImage 1:109–120.
Pozzo-Miller LD, Inoue T, DiEuliis Murphy D (1999a) Estradiol increases spine density and NMDA-dependent Ca^{2+} transients in spines of CA1 pyramidal neurons from hippocampal slices. J Neurophysiol 81:1404–1411.
Pozzo-Miller LD, Gottschalk W, Zhang L, McDermott K, Du J, Gopalakrishnan R, Oho C, Sheng Z-H, Lu B (1999b) Impairments in high-frequency transmission, synaptic vesicle docking, and synaptic vesicle distribution in the hippocampus of BDNF knockout mice. J Neurosci 19:4972–4983.
Pozzo-Miller LD, Connor JA, Andrews SB (2000) Microheterogeneity of calcium signalling in dendrites. J Physiol (Lond) 525:53–61.
Pyle JL, Kavalali ET, Piedras-Rentería ES, Tsien RW (2000) Rapid reuse of readily releasable pool vesicles at hippocampal synapses. Neuron 28:221–231.
Rutherford LC, Nelson SB, Turrigiano GC (1998) BDNF has opposite effects on the quantal amplitude of pyramidal and interneuron excitatory synapses. Neuron 21:521–530.
Ryan TA, Reuter H, Smith SJ (1997) Optical detection of a quantal presynaptic membrane turnover. Nature 388:478–482.
Schikorski T, Stevens CF (1997) Quantitative ultrastructural analysis of hippocampal excitatory synapses. J Neurosci 17:5858–5867.
Schinder AF, Poo M-m (2000) The neurotrophin hypothesis for synaptic plasticity. Trends Neurosci 23:639–645.
Schinder AF, Berninger B, Poo M-m (2000) Postsynaptic target specificity of neurotrophin-induced presynaptic potentiation. Neuron 25:151–163.
Segal RA, Greenberg ME (1996) Intracellular signaling pathways activated by neurotrophic factors. Annu Rev Neurosci 19:463–489.
Shelton DL, Sutherland J, Gripp J, Camerato T, Armanini MP, Phillips HS, Carroll K, Spencer SD, Levinson AD (1995) Human trks: molecular cloning, tissue distribution, and expression of extracellular domain immunoadhesins. J Neurosci 15:477–491.
Shepherd GMG, Harris KM (1998) Three-dimensional structure and composition of CA3–CA1 axons in rat hippocampal slices: implications for presynaptic connectivity and compartmentalization. J Neurosci 18:8300–8310.
Sherwood NT, Lo DC (1999) Long-term enhancement of central synaptic transmission by chronic brain-derived neurotrophic factor treatment. J Neurosci 19:7025–7036.
Shimada A, Mason CA, Morrison ME (1998) TrkB signaling modulates spine density and morphology independent of dendrite structure in cultured neonatal Purkinje cells. J Neurosci 18:8559–8570.
Stevens CF, Sullivan JM (1998) Regulation of the readily releasable vesicle pool by protein kinase C. Neuron 21:885–893.
Stevens CF, Tsujimoto T (1995) Estimates for the pool size of releasable quanta at a single central synapse and for the time required to refill the pool. Proc Natl Acad Sci USA 92:846–849.
Stevens CF, Williams JH (2000) "Kiss and run" exocytosis at hippocampal synapses. Proc Natl Acad Sci USA 97:12828–12833.
Stoppini L, Buchs L-A, Muller D (1991) A simple method for organotypic cultures of nervous tissue. J Neurosci Methods 37:173–182.
Südhof TC (2000) The synaptic vesicle cycle revisited. Neuron 28:317–320.
Tapley P, Lamballe F, Barbacid M (1992) K252a is a selective inhibitor of the tyrosine protein kinase activity of the trk family of oncogenes and neurotrophin receptors. Oncogene 7:371–381.
Thoenen H (1995) Neurotrophins and neuronal plasticity. Science 270:593–596.
Van der Kloot W (1991) The regulation of quantal size. Prog Neurobiol 36:93–130.
Vicario-Abejon C, Collin C, McKay RD, Segal M (1998) Neurotrophins induce formation of functional excitatory and inhibitory synapses between cultured hippocampal neurons. J Neurosci 18:7256–7271.
von Gersdorff H, Vardi E, Matthews G, Sterling P (1996) Evidence that vesicles on the synaptic ribbon of retinal bipolar neurons can be rapidly released. Neuron 116:1221–1227.
Waters J, Smith SJ (2000) Phorbol esters potentiate evoked and spontaneous release by different presynaptic mechanisms. J Neurosci 20:7863–7870.
Xu B, Gottschalk W, Chow A, Wilson RI, Schnell E, Zang K, Wang D, Nicoll RA, Lu B, Reichardt LF (2000) The role of brain-derived neurotrophic factor receptors in the mature hippocampus: modulation of long-term potentiation through a presynaptic mechanism involving TrkB. J Neurosci 20:6888–6897.
Zucker RS (1989) Short-term synaptic plasticity. Annu Rev Neurosci 12:13–31.
Zucker RS (1996) Exocytosis: a molecular and physiological perspective. Neuron 17:1049–1055.